



Measurement and model calculation of the temperature dependence of ligand-to-metal energy transfer rates in lanthanide complexes

Wagner M. Faustino^{a,*}, Luiz A. Nunes^b, Idelma A.A. Terra^b, Maria Claudia F.C. Felinto^c, Hermi F. Brito^d, Oscar L. Malta^e

^a Departamento de Química, Universidade Federal da Paraíba, 58051-970, João Pessoa PB, Brazil

^b Instituto de Física, Universidade de São Paulo, 13560-970 São Carlos SP, Brazil

^c IPEN, 05505-800 São Paulo SP, Brazil

^d Instituto de Química, Universidade de São Paulo, 05508-900 São Paulo SP, Brazil

^e Departamento de Química Fundamental, Universidade Federal de Pernambuco, 50670-901, Recife PE, Brazil

ARTICLE INFO

Article history:

Received 12 September 2012

Received in revised form

7 January 2013

Accepted 9 January 2013

Available online 18 January 2013

Keywords:

Lanthanide coordination compounds

Energy transfer

Transients

ABSTRACT

Temperature dependent transient curves of excited levels of a model Eu^{3+} complex have been measured for the first time. A coincidence between the temperature dependent rise time of the $^5\text{D}_0$ emitting level and decay time of the $^5\text{D}_1$ excited level in the $[\text{Eu}(\text{tta})_3(\text{H}_2\text{O})_2]$ complex has been found, which unambiguously proves the $\text{T}_1 \rightarrow ^5\text{D}_1 \rightarrow ^5\text{D}_0$ sensitization pathway. A theoretical approach for the temperature dependent energy transfer rates has been successfully applied to the rationalization of the experimental data.

© 2013 Elsevier B.V. All rights reserved.

1. Introduction

Intramolecular energy transfer is a process of paramount importance in describing the luminescence behavior of lanthanide coordination compounds. Emission quantum yields of 4f–4f transitions can be considerably increased when the compound is excited through the ligands, instead of direct excitation of the lanthanide 4f states. This phenomenon was first rationalized by Weissman in 1942 in terms of ligand-to-metal intramolecular energy transfer in trivalent europium coordinated by organic ligands [1]. Since then, the enormous amount of data appearing in the literature [2–7] on the luminescence properties of this type of compound has been interpreted in terms of this process. The theoretical challenge of describing intramolecular energy transfer processes that occur between a ligand and a lanthanide ion in luminescent complexes, including selection rules, was first treated in detail in references [5,8]. Expressions for transfer rates corresponding to the so-called direct Coulomb and exchange mechanisms have been obtained, from which selection rules could be derived [9].

Trivalent europium is extremely useful in studying and testing intramolecular energy transfer models due to the special characteristics of its energy level structure. The energies of the excited

$^5\text{D}_j$ manifolds ($J=0-4$) of the $4f^6$ configuration are sufficiently well separated from the ground state $^7\text{F}_j$ manifolds ($J=0-6$) and usually present appropriate resonance conditions with excited states of the ligands. In this case most of the experimental data has been interpreted in terms of energy transfer from the lowest triplet states of the ligands (T_1) to the $^5\text{D}_j$ manifolds, particularly the $^5\text{D}_0$ and $^5\text{D}_1$ excited states, following absorption from the singlet ground state (S_0) to either the lowest excited singlet state (S_1) or the $^5\text{L}_6$ 4f level that after populate the T_1 state in the ligands via respectively intersystem crossing or energy transfer [1–6], even though direct intramolecular energy transfer from S_1 to excited states of the lanthanide is also possible in some cases [10]. The experimental measurements to get information on the transfer channels have been based either on the behavior of the T_1 phosphorescence, from gadolinium compounds with large energy gap (Gd^{3+} : $^7\text{P}_{7/2} \rightarrow ^8\text{S}_{7/2} \sim 32000 \text{ cm}^{-1}$), mainly, and/or the rise-times of the luminescence transient curves of the lanthanide emitting levels. The interpretation of the results becomes rather delicate when mixed ligands, having close excited states, are coordinated to the lanthanide ion. Since both the transient and the steady-state regime emission quantum yield is the result of a balance between absorption, decay rates (radiative and non-radiative) and intramolecular energy transfer rates, the treatment of an appropriate system of rate equations for each case can indicate which energy transfer channels are actually operative. This presumes the knowledge of energy transfer mechanisms (transfer rate values) and the associated selection rules, an aspect

* Corresponding author. Tel.: +55 83 3216 7591; fax: +55 83 3216 7437.

E-mail address: wmafastino@yahoo.com.br (W.M. Faustino).

that has not been taken into consideration in these experimental works reported in the literature. Furthermore, the dependence of intramolecular energy rates with temperature has been overlooked.

The aim of the present work is to report for the first time – to the best of our knowledge – a direct measurement of temperature dependent intramolecular energy transfer rates in a lanthanide complex. The ligand T_1 triplet to the 5D_1 state of the Eu^{3+} ion energy transfer rate was measured by using time resolved spectroscopy in the nano- and micro-second scales. The experiment was planned with the objective of testing predictions made by the theoretical approach developed previously concerning energy transfer mechanisms, selection rules and temperature dependence of transfer rates [8,11]. The complex $[\text{Eu}(\text{tta})_3(\text{H}_2\text{O})_2]$ (tta =thenoyltrifluoroacetate) was chosen as a model system due to the following reasons: (i) only one type of organic ligand is present; (ii) the complex has been characterized spectroscopically and theoretical studies on coordination geometry optimization and on electronic structure have been carried out previously [5]; and (iii) the tta S_1 singlet state is energetically distant from the Eu^{3+} 5D_0 and 5D_1 states ($> 7000 \text{ cm}^{-1}$), while the triplet T_1 barycenter is located below the 5D_2 and slightly above the 5D_1 state ($\sim 400 \text{ cm}^{-1}$).

2. Experimental section

The $[\text{Eu}(\text{tta})_3(\text{H}_2\text{O})_2]$ complex was prepared by the method described by Charles and Ohlmann [12]. The C and H contents were obtained via conventional elemental analysis and the Eu^{3+} content via complexometric titration with EDTA. The percentages found (calculated) were C: 33.88 (33.85); H: 1.88 (1.89); Eu: 17.76 (17.85), corresponding to the general formula $\text{C}_{24}\text{H}_{16}\text{F}_9\text{O}_8\text{S}_3\text{Eu}$.

The luminescence spectra in the visible range from 520 to 630 nm were obtained using a laser HeCd (Kimmon/IK5652R-G) at 325 nm as the excitation source and were taken at different temperatures (between 10 and 300 K). The luminescence signals were dispersed by a double monochromator (0.85 m, SPEX 1403) equipped with a photomultiplier tube (Hamamatsu/R928), amplified by a lock-in amplifier (Stanford Research systems/SR 830 DSP) and recorded by a computer.

The luminescence transient measurements were performed by using the third harmonic (355 nm) of a Nd-YAG laser (Surelite I/Continuum, 10 Hz, 5 ns) as the excitation source. The transient signals were dispersed by the same double monochromator equipped with a photomultiplier tube and were recorded with a digital oscilloscope (TekTronix/TDS380) at temperatures from 10 to 300 K. The temporal resolution of the electronic module was about 10 ns. The temperature dependent data were measured by using a Janis Helium Flux Cryostat.

3. Theoretical approach

According to Fermi's golden rule, the energy transfer rate from an excited donor state D^* to an excited acceptor A^* , is given by

$$W_{ET} = \frac{2\pi}{\hbar} |\langle A^*D | H | AD^* \rangle|^2 F \quad (1)$$

where the matrix element corresponds to either direct or exchange electronic interactions between donor and acceptor states, and the temperature dependent factor F corresponds to their spectral overlap (resonance condition). In the case investigated here the donor state corresponds to a ligand centered state labeled as $|\phi^*\rangle$, and the acceptor state corresponds to a lanthanide centered 4f state labeled as $|\psi'JM\rangle$ as indicated in Fig. 1. If only the direct coulomb interaction is operative the energy

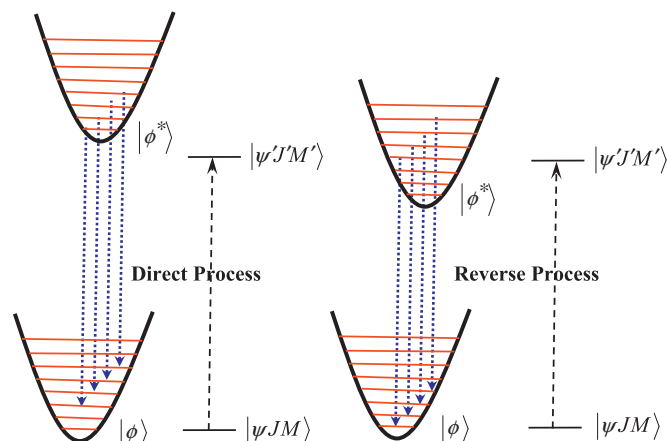


Fig. 1. Configurational coordinate diagrams for direct and reverse thermally activated ligand-to-metal energy transfer processes.

transfer rate is given by [8,9]

$$W_{ET}^C = \frac{e^2 S_L F}{G(2J+1)} \sum_{\lambda=2,4,6} \left(\frac{\Omega_{\lambda}^{e,d}}{R_L^6} + \frac{(\lambda+1)\langle r^{\lambda} \rangle \langle 3\|C^{(\lambda)}\|3 \rangle^2 (1-\sigma_{\lambda})^2}{(R_L^{\lambda+2})^2} \right) \langle \alpha'J' \| U^{(\lambda)} \| \alpha J \rangle^2 \quad (2)$$

where S_L stands for the dipole strength of the intraligand transition $|^3\pi^*\rangle \rightarrow |^1\pi\rangle$, G stands for degeneracy of the donor state, and $\Omega_{\lambda}^{e,d}$ ($\lambda=2, 4$ and 6) stands for the forced electric dipole contribution to the so-called 4f–4f intensity parameters described by the Judd–Ofelt theory [13,14]. The donor–acceptor distance, R_L (often between 3 and 5 Å), is taken as the distance from the lanthanide nucleus to the barycenter of the ligand electronic state involved in the energy transfer process. The eigenfunctions are taken in the intermediate coupling scheme, in which J is assumed as a good quantum number, approximately. The lanthanide 4f radial integrals $\langle r^{\lambda} \rangle$ and reduced matrix elements are available in the literature [8] and references therein.

On the other hand, if only the exchange interaction is operative the energy transfer rate is given by [8]

$$W_{ex} = \frac{\langle 4f|L\rangle^4}{(2J+1)} \frac{8\pi e^2}{3\hbar R_L^4} \langle \psi'J' \| S \| \psi J \rangle^2 \sum_m |\langle \phi | \sum_j \mu_z(j) s_m(j) | \phi^* \rangle|^2 F \quad (3)$$

where s_m ($m=-1, 0, 1$) is the spherical component of the spin operator of electron j in the ligand, μ_z is the z-component of its dipole operator and S is the total spin operator of the lanthanide ion. Typical values of the squared matrix element of the coupled dipole and spin operators in Eq.(3) are in the range 10^{-34} – 10^{-36} (e.s.u.) $^2\text{cm}^2$ [8,9]. This coupled operator breaks down the usual selection rules in the singlet–singlet and singlet–triplet matrix elements. An important aspect in Eq. (2) is that shielding effects produced by the filled 5s and 5p sub-shells are taken into account through the Sternheimer's shielding factors σ_k . These factors are taken into account by the fact that the donor ligand state feels this shielding effect in a multipolar interaction, according to the present model, in contrast to the case of the exchange interaction, where the donor–acceptor overlap integral naturally includes this effect. An analytical formulation for these factors has been given in Ref. [8].

The quantity $\langle 4f|L\rangle$ is the radial overlap integral between the 4f sub-shell and the ligand eigenfunction ϕ^* centered at a distance R_L , as mentioned above. This overlap is certainly difficult to estimate. It should be small, less than 0.05, the typical value of the total overlap between 4f orbitals and the ligating atom. Within our purposes we have considered values between 0.04

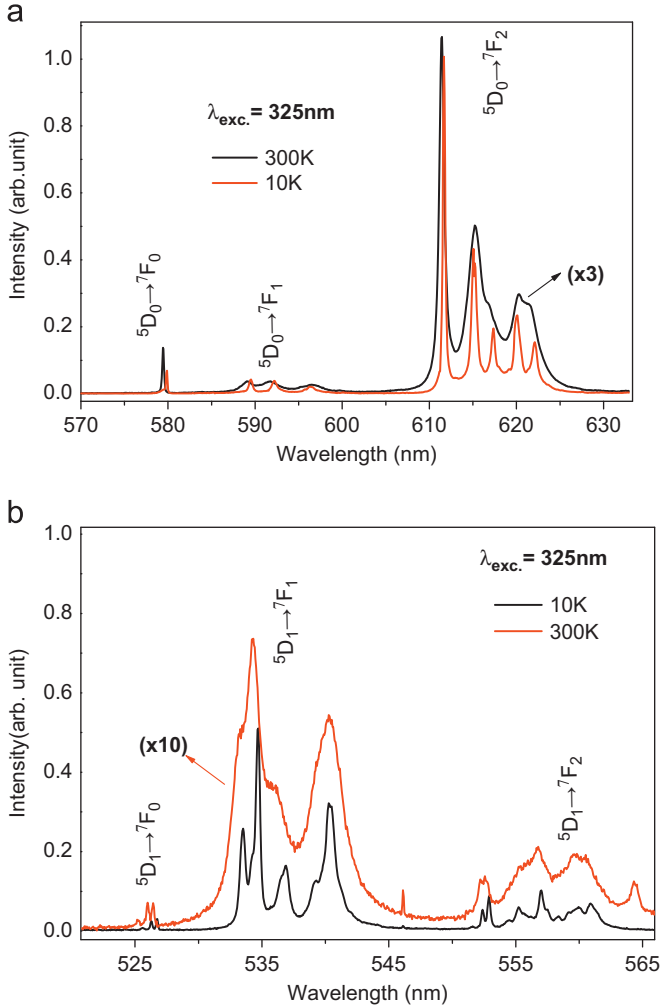


Fig. 2. Emission spectra of the $[\text{Eu}(\text{tta})_3(\text{H}_2\text{O})_2]$ complex recorded at 10 and 300K: (a) ${}^5\text{D}_0 \rightarrow {}^7\text{F}_{0-4}$ transitions and (b) ${}^5\text{D}_1 \rightarrow {}^7\text{F}_{0-2}$ transitions. The emission intensities of the ${}^5\text{D}_0 \rightarrow {}^7\text{F}_j$ transitions are stronger than those arising from the ${}^5\text{D}_1$ level by a factor of 10^3 .

and 0.03, which are reliably acceptable taking into account that the molecular ligand excited states are quite delocalized.

A point of high importance, as it can be derived from Eq. (3), is the selection rule associated to the ${}^5\text{D}_0$ and ${}^5\text{D}_1$ levels of the Eu^{3+} ion. According to the reduced matrix element of the lanthanide spin operator $\Delta J=0, \pm 1$ ($J=J=0$ excluded). This means that energy transfer to the ${}^5\text{D}_0$ level, the Eu^{3+} ion being initially in the ${}^7\text{F}_0$ ground state, by the exchange mechanism, is forbidden, even though this selection rule might be relaxed if the ${}^7\text{F}_1$ level is thermally populated at high temperatures. Besides, this energy transfer process is also forbidden by the dipole–dipole and dipole–multipole mechanisms, according to the reduced matrix elements of the unit tensor operator $\mathbf{U}^{(\lambda)}$, as far as J -mixing effects, which are small, are neglected.

The calculation of F factor is based on the methodology described in Ref. [11] and starts from the energy level diagrams shown in Fig. 1. Energy conservation implies phonon creation when $|\psi'JM\rangle$ is below the donor state, and phonon annihilation in the opposite case.

From these facts, and assuming a Boltzmann distribution for the vibrational components of the electronic states, one may show that [11]

$$F \approx \sum_{m,m',n,n'} (1 - e^{-\hbar\omega_{\phi^*}/kT}) e^{-m\hbar\omega_{\phi^*}/kT} \langle \chi_m^{\phi^*} | \chi_m^{\phi} \rangle^2 (1 - e^{-\hbar\omega_j/kT}) e^{-n\hbar\omega_j/kT}$$

$$\langle t_n^j | t_n^j \rangle^2 \int g_n^j(E) g_m^{\phi^*}(E) dE dE' \times \delta(\Delta E + m\hbar\omega_{\phi} - m'\hbar\omega_{\phi^*} - n'\hbar\omega_j + n\hbar\omega_j) \quad (4)$$

where $\chi_i^{\phi^*}$, χ_i^{ϕ} , t_i^j and t_i^j are vibrational components, with frequencies ω_{ϕ} , ω_{ϕ^*} , ω_j and ω_j , respectively to the electronic states $|\phi\rangle$, $|\phi^*\rangle$, $|\psi JM\rangle$ and $|\psi'JM\rangle$, respectively, and ΔE is the zero-point energy difference between the donor and acceptor states. $g_n^j(E)$ and $g_m^{\phi^*}(E)$ are the band-shapes of the vibronic components of the 4f and intraligand states, respectively.

By considering that $\langle t_n^j | t_n^j \rangle = \delta_{n,n'}$, which is an approximation often assumed in lanthanide spectroscopy, and that both parabolas shown in Fig. 1 have approximately the same curvature, one may show that

$$F \approx \sum_{m,m'} (1 - e^{-\hbar\omega_{\phi}/kT}) e^{-m\hbar\omega_{\phi}/kT} \langle \chi_m^{\phi^*} | \chi_m^{\phi} \rangle^2 \int \times \left[\sum_n (1 - e^{-\hbar\omega_j/kT}) e^{-n\hbar\omega_j/kT} g_n^j(E) \right] g_m^{\phi^*}(E) dE dE' \times \delta(\Delta E + (m - m')\hbar\omega_{\phi}) \quad (5)$$

In Eq. (5), the term in brackets corresponds to the band-shape function for the electronic transition $|\psi'JM\rangle \rightarrow |\psi JM\rangle$, $G^j(E)$, which might be approximated by a Gaussian function [11]. This type of band-shape was also chosen for each vibronic component of the state $|\phi^*\rangle$. Thus, it may be shown that

$$F \approx \bar{F} \sum_{i=\max(0,n_p)} (1 - e^{-\hbar\omega_{\phi}/kT}) e^{-i\hbar\omega_{\phi}/kT} \langle \chi_{i-n_p}^{\phi^*} | \chi_i^{\phi} \rangle^2 \quad (6)$$

where $n_p \approx \Delta E/\hbar\omega_0$ phonons are created, if $\Delta E \leq 0$, or annihilated, if $\Delta E \geq 0$, in the energy transfer process. \bar{F} is an overlap integral between two Gaussian functions, and is given by [9,11]

$$\bar{F} = \frac{\ln 2}{\sqrt{\pi}} \frac{1}{\hbar^2 \gamma_{Af} \gamma_{vib}} \{ [(1/\hbar\gamma_{vib})^2 + (1/\hbar\gamma_{Af})^2] \ln 2 \}^{1/2} \times \exp \left(\frac{1}{4} \frac{((2\Delta/\hbar\gamma_{Af})^2 \ln 2)^2}{[(1/\hbar\gamma_{vib})^2 + (1/\hbar\gamma_{Af})^2] \ln 2} - (\Delta/\hbar\gamma_{Af})^2 \ln 2 \right) \quad (7)$$

where $\hbar\gamma_{Af}$ and $\hbar\gamma_{vib}$ are the widths at half-height, respectively, of the 4f state and the vibronic component of the intraligand transition, and Δ is the dissonance between ΔE and $n_p \hbar\omega_{\phi}$.

The sum in Eq. (6) can be described as a function of the so-called Huang–Rhys parameters, S , and it may be shown that

$$F \approx \bar{F} \sum_{i=\max(0,n_p)} \frac{e^{-S\langle 2m+1 \rangle} (S\langle m \rangle)^i (S\langle 1+m \rangle)^{i-n_p}}{i!(i-n_p)!} \quad (8)$$

where $\langle m \rangle$ is the average vibrational quantum number given by

$$\langle m \rangle = \frac{\sum_m m e^{-m\hbar\omega_0/kT}}{\sum_m e^{-m\hbar\omega_0/kT}} \quad (9)$$

4. Results and discussion

Fig. 2(a) shows the emission spectrum of the $[\text{Eu}(\text{tta})_3(\text{H}_2\text{O})_2]$ complex recorded in the spectral range from 570 to 630 nm, at room and liquid helium temperatures (300 and 10 K), under excitation at 325 nm using a He–Cd pumping laser. This photoluminescence spectrum consists of the characteristic narrow bands of the Eu^{3+} ion assigned to the intraconfigurational transitions ${}^5\text{D}_0 \rightarrow {}^7\text{F}_0$ (580 nm), ${}^5\text{D}_0 \rightarrow {}^7\text{F}_1$ (590, 592 and 596 nm) and ${}^5\text{D}_0 \rightarrow {}^7\text{F}_2$ (612, 615, 617, 620 and 622 nm), exhibiting the hypersensitive ${}^5\text{D}_0 \rightarrow {}^7\text{F}_2$ transition around 612 nm as the most prominent. Fig. 2(b) presents several much less intense emission bands (by three orders of magnitude), assigned to the ${}^5\text{D}_1 \rightarrow {}^7\text{F}_0$ (526 nm), ${}^5\text{D}_1 \rightarrow {}^7\text{F}_1$ (534) and ${}^5\text{D}_1 \rightarrow {}^7\text{F}_2$ (557 nm) transitions,

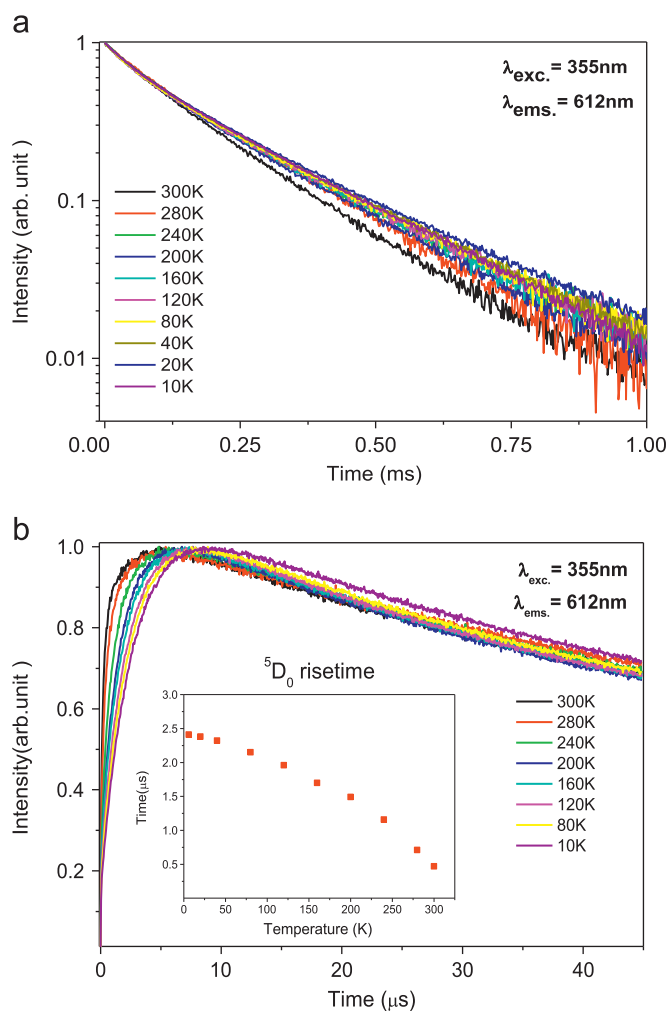


Fig. 3. Luminescence transients of the 5D_0 level of the $[\text{Eu}(\text{tta})_3(\text{H}_2\text{O})_2]$ complex recorded in the temperature interval from 10 to 300 K under excitation at 355 nm: Decay (a) and rising (b) curves of the 5D_0 level. The inset shows the plot of risetime (μs) versus temperature (K).

showing the strongest emission intensity at 534 nm. In addition, a sharp peak is observed at 564 nm in the emission spectrum recorded at 300 K. However, this peak is absent at low temperature, indicating that, at room temperature, this transition is originated from an upper 5D_1 Stark level thermally populated.

Fig. 3(a) presents the luminescence decay curves of the emitting 5D_0 level of the $[\text{Eu}(\text{tta})_3(\text{H}_2\text{O})_2]$ complex recorded at temperature interval from 10 to 300 K, under excitation at 355 nm. The 5D_0 lifetimes are in the millisecond scale; actually they are less than one millisecond (~ 0.2 ms) due to the presence of water molecules in the first coordination sphere, as expected. Fig. 3(b) shows the very initial part of the transient curves, in the microsecond scale, of this emitting level at different temperatures. The 5D_0 risetimes (shown in the inset) were obtained as the area under these curves from the initial time until the time corresponding to maximal emission intensity.

The transient luminescence curves of the 5D_1 level of the $[\text{Eu}(\text{tta})_3(\text{H}_2\text{O})_2]$ complex, recorded at several temperatures (10–300 K), are shown in Fig. 4. The decay curves also deviate from single exponentials due to intramolecular energy transfer processes [Fig. 4(a)]. The very initial part of the transient curves of the 5D_1 level, from the area under which the risetimes were obtained, are shown in Fig. 4(b). To the best of our knowledge, it is the first time that direct measurements of these risetimes in an europium complex at different temperatures were carried out.

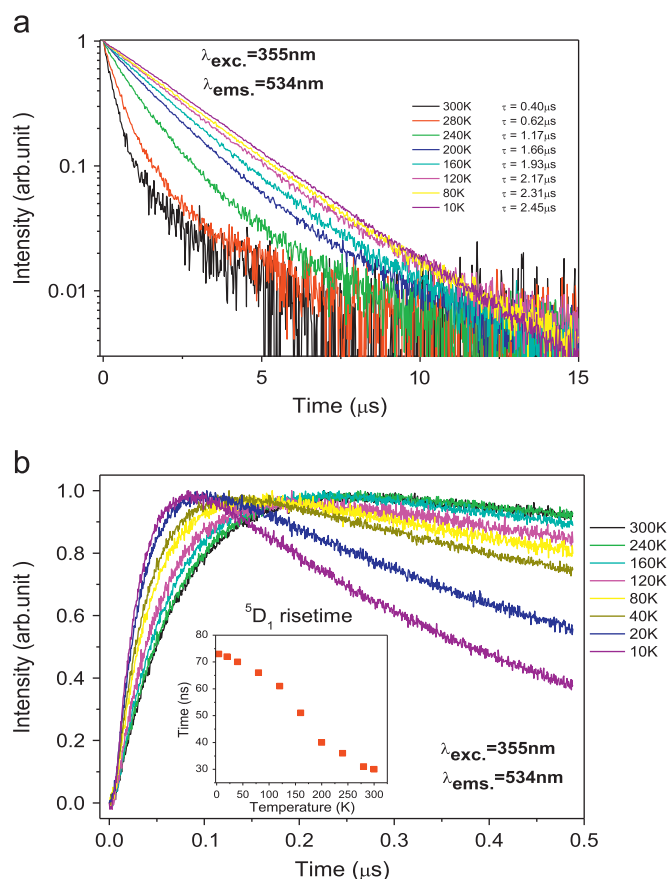


Fig. 4. Luminescence transients of the 5D_1 level of the $[\text{Eu}(\text{tta})_3(\text{H}_2\text{O})_2]$ complex recorded in the temperature interval from 10 to 300 K: Decay (a) and rising (b) curves of the 5D_1 level. The inset presents the plot of risetime (μs) versus temperature (K).

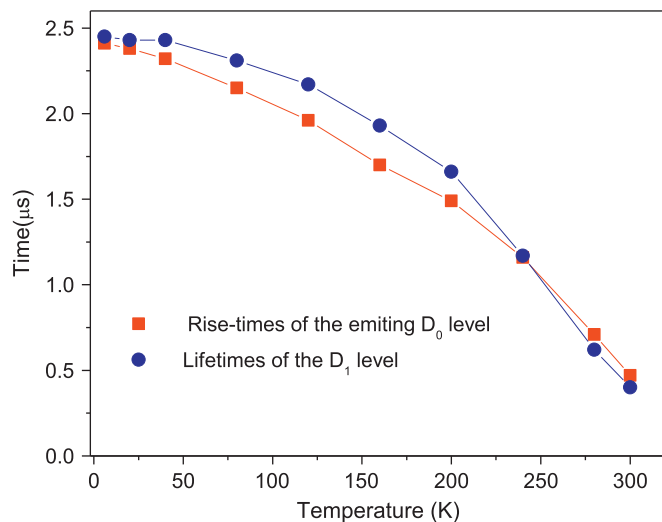


Fig. 5. Luminescence lifetimes of the 5D_1 level and risetimes of the 5D_0 level of the $[\text{Eu}(\text{tta})_3(\text{H}_2\text{O})_2]$ complex as a function of temperature.

Fig. 5 shows both the risetime of the emitting 5D_0 and the lifetime of the 5D_1 level at different temperatures. For each temperature these characteristic times are practically the same, which indicates that the 5D_0 is populated directly from the 5D_1 level.

The theoretical approach developed in the previous section has been applied to the analysis of the experimental results shown

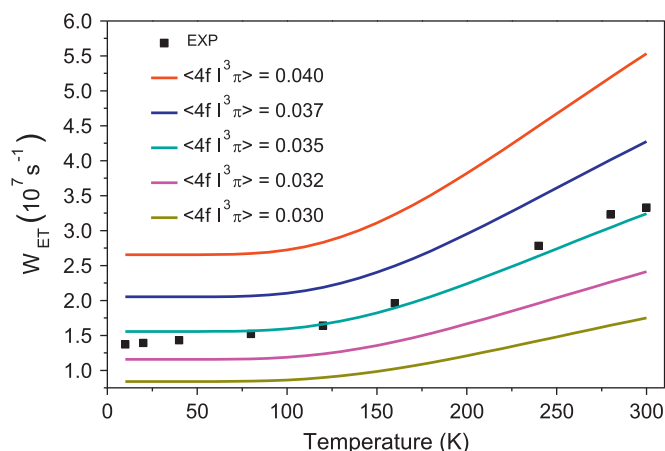


Fig. 6. Experimental and theoretical energy transfer rates from the triplet state (T_1) to the 5D_1 level of the $[\text{Eu}(\text{tta})_3(\text{H}_2\text{O})_2]$ complex. The theoretical curves correspond to different values of the overlap integral in Eq. 3.

above. In our analysis, we have considered only the temperature dependent energy transfer rates from the triplet states to the 5D_1 level since our experimental results indicate that the 5D_0 is not efficiently populated from any level different from the 5D_1 . The phonon energy was assumed to be $\sim 400 \text{ cm}^{-1}$, which is typical for the vibrational stretching $\text{Ln}^{3+}-\text{O}$ in diketonate complexes [11] and in the calculations we have assumed $\hbar\gamma_{\text{vibCT}} \sim 50 \text{ cm}^{-1}$. The Huang–Rhys parameter was evaluated as 6.25, by considering the band width for the triplet state $\sim 3000 \text{ cm}^{-1}$. The experimental energy transfer rates $T \rightarrow {}^5D_1$ were assumed to be the inverse of the risetime of the 5D_1 level obtained from Fig. 4(b). Theoretical and experimental temperature dependent energy

transfer rates from the triplet state to the 5D_1 level of the $[\text{Eu}(\text{tta})_3(\text{H}_2\text{O})_2]$ complex are shown in Fig. 6.

Good agreement between the theoretical and experimental profiles of the temperature dependent energy transfer rates from the triplet state to the 5D_1 level of the $[\text{Eu}(\text{tta})_3(\text{H}_2\text{O})_2]$ complex is obtained. This agreement strongly indicates that the luminescence sensitization of the Eu^{3+} ion in the complex is dominated by the $T \rightarrow {}^5D_1 \rightarrow {}^5D_0$ path. This mechanism, which is qualitatively discussed in many papers reporting on luminescent europium complexes, was also recently corroborated by Ha-Thi et al. [15].

In conclusion, the temperature dependent transient curves of the 5D_1 and 5D_0 levels in a model Eu^{3+} complex, reported here, for the first time, have been used along with a theoretical approach for the temperature dependent energy transfer rates to corroborate the $T_1 \rightarrow {}^5D_1 \rightarrow {}^5D_0$ luminescence sensitization pathway.

References

- [1] S.I. Weissman, J. Chem. Phys. 10 (1942) 214.
- [2] R.E. Whan, G.A. Crosby, J. Mol. Spectrosc. 8 (1962) 315.
- [3] S.P. Sinha, Europium, Springer-Verlag, New York, 1967.
- [4] N. Sabbatini, M. Guardigli, J.M. Lehn, Coord. Chem. Rev. 123 (1993) 201.
- [5] G.F. de Sá, O.L. Malta, C. de Mello Donegá, A.M. Simas, R.L. Longo, P.A. Santa-Cruz, E.F. da Silva Jr., Coord. Chem. Rev. 196 (2000) 165.
- [6] J.-C.G. Bünzli, A.-S. Chauvin, H.K. Kim, E. Deiters, S.V. Eliseeva, Coord. Chem. Rev. 254 (2010) 2623.
- [7] K. Binnemans, Chem. Rev. 109 (2009) 4374.
- [8] O.L. Malta, J. Non-Cryst. Solids 354 (2008) 4770.
- [9] O.L. Malta, J. Lumin. 71 (1997) 229.
- [10] M. Klainerman, J. Chem. Phys. 51 (1969) 2370.
- [11] W.M. Faustino, O.L. Malta, G.F. de Sa, Chem. Phys. Lett. 429 (2006) 595.
- [12] R.G. Charles, R.C. Ohlmann, J. Inorg. Nucl. Chem 27 (1965) 255.
- [13] B.R. Judd, Phys. Rev. 127 (1962) 750.
- [14] G.S. Ofelt, J. Chem. Phys. 37 (1962) 511.
- [15] M.-H. Ha-Thi, J.A.A. Delaire, V. Michelet, I. Leray, J. Phys. Chem. A. 114 (2010) 3264.